Co-published by
Institute of Fluid-Flow Machinery
Polish Academy of Sciences
Committee on Thermodynamics and Combustion
Polish Academy of Sciences

http://www.imp.gda.pl/archives-of-thermodynamics/

Thermodynamic modelling and experimental validation of direct carbon dioxide methylation to para-xylene

Xiaofeng Du

Beijing District Heating Group Co., Ltd., Fengtai Branch, Building 3, Zone 1, Zifangyuan, Fengtai District, Beijing 100161, China
Author email: dxf851021@163.com

Received: 09.06.2025; revised: 29.10.2025; accepted: 18.11.2025

Abstract

With the acceleration of global industrialisation, carbon dioxide (CO_2) emissions continue to rise, causing a series of environmental problems. The development of CO_2 conversion and utilisation technology is of great significance for achieving sustainable development. This study conducts an in-depth thermodynamic analysis of the key reactions in the CO_2 conversion and utilisation process based on the principle of thermodynamic equilibrium. By constructing a chemical reaction model, thermodynamic parameters such as equilibrium constants and Gibbs free energy are calculated for various reactions under different temperature and pressure conditions, and the feasibility and product distribution of the reactions are evaluated. Meanwhile, the influence of different reaction conditions on the distribution of equilibrium products during CO_2 conversion and utilisation is explored. The results showed that under the conditions of 370−440°C, 3 MPa, and a feed molar ratio (1:1−1:4), the conversion rate of CO_2 and toluene was over 90%, and the selectivity of xylene was over 60%. From thermodynamic analysis, the order of thermodynamic advantages of the entire reaction was: CH_3OH methylation > CO_2 methylation > CO_2 to olefin production. Based on the above data, the optimal operating parameters for the CO_2 direct methylation process were determined through thermodynamic analysis. This study can provide an important theoretical basis and practical guidance for the industrial application of CO_2 conversion and utilisation technology.

Keywords: CO_2 conversion and utilisation; Thermodynamic analysis; Key conversion reactions; Catalyser; Reaction mechanism

Vol. 46(2025), No. 4, 215–228; doi: 10.24425/ather.2025.156851

Cite this manuscript as: Du, X. (2025). Thermodynamic modelling and experimental validation of direct carbon dioxide methylation to para-xylene. *Archives of Thermodynamics*, 46(4), 215–228.

1. Introduction

With the acceleration of global industrialisation, energy-related carbon dioxide (CO_2) emissions continue to rise. The global CO_2 emissions in 2022 have reached 36.8 billion tons. If effective measures are not taken, it is expected that the global temperature rise will exceed 2°C by the end of the 21st century, triggering extreme climate and ecological crises [1]. In this context, CO_2 resource utilisation technology has become an international research hotspot, with the goal of converting CO_2 into high value-added chemicals (such as methanol, olefins, aromatics, etc.), achieving a carbon cycle loop and benefits win-win situation. In recent years, the direct methylation of CO_2 to produce p-xylene (PX) has attracted much attention due to its strategic position in the aromatic hydrocarbon industry chain. However, this process faces thermodynamic limitations, competition from side reactions and catalyst design bottlenecks, which urgently require systematic thermodynamic analysis and process optimisation [2]. Many experts and scholars have conducted research and analysis on this. Guo et al. [3] developed a metal oxide/zeolite bifunctional catalyst to improve the efficiency of CO_2 hydrogenation to aromatics and studied it using the ZnZrOx/ZSM-5 system as an example. This sys-

Nomenclature

f_i – fugacity of the *i*-th substance, Pa
f_i^0 – standard fugacity of the *i*-th substance, Pa
G^t – total Gibbs free energy of the system, kJ/mol
G_r^0 – standard Gibbs free energy of the *i*-th substance
ΔG – Gibbs free energy change, kJ/mol
ΔG_r^0 – standard molar Gibbs free energy change of reaction, kJ/mol
ΔH – enthalpy change, kJ/mol
ΔH_r^0 – standard molar enthalpy change of reaction, kJ/mol
K – equilibrium constant
K^0 – standard equilibrium constant
n_i – number of moles of the *i*-th substance
N – number of reactants
R – ideal gas constant, = 8.3145 J/(mol K)
ΔS – entropy change, kJ/(mol K)
ΔS_r^0 – standard molar entropy change of reaction, kJ/(mol K)
T – temperature, K
T^0 – standard temperature, K

Greek symbols

η_{co_2} – CO_2 conversion rate
η_T – toluene conversion rate
Ψ_i – distribution ratio of the *i*-th substance

Abbreviations and Acronyms

C1-C4 – carbon number 1 to 4 hydrocarbons
C^{9+} – carbon number ≥ 9 aromatic hydrocarbons
GFE – Gibbs free energy
HZSM-5 – proton-exchanged zeolite socony Mobil-5
MOX – metal oxides
MTA – methanol-to-aromatics
MTO – methanol-to-olefins
PX – p-xylene
SX – selectivity of xylene
ZnZrOx – zinc-zirconium oxide
$ZnCr_2O_4$ – zinc chromite
ZrCuOx – zirconium-copper oxide
ZSM-5 – zeolite socony Mobil-5

tem could achieve a CO_2 conversion rate of over 30%, demonstrating the development potential of bifunctional catalysts in CO_2 hydrogenation to aromatics. Qi et al. [4] explored the laws and limiting factors of the CO_2 methylation reaction through thermodynamic calculations. It was found that the reaction is limited by Gibbs free energy (GFE), and low temperature (< 400°C) conditions are more conducive to the generation of PX. This achievement provided a theoretical basis for optimising the reaction conditions of CO_2 hydrogenation to aromatics from a thermodynamic perspective, and clarified the importance of temperature control for the generation of the target product PX. Wang et al. [5] found that zeolite acidity regulation can effectively inhibit the isomerisation reaction of PX, which has a positive significance for improving the selectivity of PX. However, despite acidity regulation, the selectivity of by-product light hydrocarbons (C_1-C_4) in the CO_2 hydrogenation to aromatics process was still as high as 40%. This indicated that there were still challenges in inhibiting side reactions and improving the selectivity of target products. Ma and Liu [6] compared the efficiency of different metal oxides in CO_2 activation and found that metal oxides, such as ZrCuOx, had significantly better CO_2 activation efficiency than traditional Cu/ZnO systems. Awad et al. [7] studied the reaction of CO_2 hydrogenation to aromatics under different pressure conditions and found that high-pressure operation (3–5 MPa) can improve the conversion rate of raw materials, but at the same time, energy consumption will also increase. This required a balance between the advantages and disadvantages of high-pressure operation in practical applications. On the one hand, increasing pressure could promote the reaction towards generating more aromatic products and improve the utilisation efficiency of raw materials. However, excessive pressure could lead to an increase in equipment investment costs and energy consumption, thereby affecting the economic feasibility of the entire process. Kim et al. [8] conducted process integration research and proposed a strategy for unreacted gas circulation. This strategy could increase carbon utilisation to 70%. This was of great significance for improving the resource utilisation efficiency of the CO_2 hydrogenation to aromatics process. By recycling unreacted gases, not only was the utilisation rate of raw materials increased and waste emissions reduced, but also production costs were lowered. Zheng et al. [9] conducted an economic evaluation and found that the production cost of PX is extremely sensitive to the lifespan of the catalyst. PX production was only competitive when the lifespan of the catalyst exceeded 1000 hours. This highlighted the crucial role of catalyst stability in the industrial production of aromatics through CO_2 hydrogenation. Long-life catalysts could reduce the cost of frequent catalyst replacement, minimise production interruptions caused by catalyst deactivation, and ensure production continuity and economy. Xu et al. [10] studied the indirect pathway of CO_2 and found that although this pathway is relatively mature, it is prone to trigger side reactions in methanol-to-olefins (MTO). This meant that when using indirect pathways for CO_2 hydrogenation to produce aromatics, it was necessary to pay attention to and solve the problems caused by side reactions, such as decreased product selectivity and increased separation costs. However, due to its relatively mature technology, it still had some practical value.

The above studies show that single reaction pathway analysis cannot reveal the mechanism of side reaction competition. Pure experimental research lacks thermodynamic guidance and is difficult to systematically optimise. The dynamic model relies on reaction mechanism parameters that cannot be clearly defined. In view of this, the study adopts thermodynamic equilibrium analysis based on the GFE minimisation principle, and combines Advanced System for Process Engineering Plus (ASPEN Plus) with Python coupling calculation to construct a CO_2 conversion system model containing 17 main/side reactions. This method can systematically analyse the competition and cooperation relationships between pathways in complex reaction networks and predict the equilibrium composition by minimising the total GFE of the system. It uses ASPEN Plus's reliable physical property database and Python's flexible scalability to implement multi-condition optimisation calculations.

At the same time, the model's accuracy is verified through experimental data.

The main innovation of the research lies in the construction of a CO_2 conversion system model based on the GFE minimisation principle, which includes 17 main/side reactions. Through ASPEN Plus and Python coupling calculation, the thermodynamic parameters of each reaction under standard conditions are quantified, and the thermodynamic advantage order of 'methanol methylation > CO_2 methylation > CO_2 to olefins' is clarified. At the same time, the limitations of single factor analysis are broken through, systematically exploring the synergistic effects of temperature, pressure and feed ratio, and determining the optimal process parameters of 370−440°C, 3 MPa, CO_2/C_7H_8 = 1:1−1:4.

Compared to previous research, it has solved multiple problems. One reason is that previous studies have focused on a single reaction pathway and have not clearly defined the conditions for inhibiting side reactions. This study explains the impact of side reaction competition on PX selectivity through the 17 reaction model. The second is to solve the problem of the disconnect between catalyst design and thermodynamic optimisation. Previous studies did not relate thermodynamic characteristics to catalyst deactivation. Based on the endothermic characteristics of the toluene disproportionation side reaction, this study specifically designs a bifunctional catalyst. The third is to quantify the applicable scenarios of 'direct/indirect methylation'.

2. Methods and materials

2.1. CO_2 conversion scheme and materials

As global climate change becomes increasingly severe, reducing CO_2 emissions has become a shared responsibility of the international community. In this context, global researchers have conducted numerous studies on developing efficient and economically feasible CO_2 capture and utilisation technologies. Especially, the methylation reaction between CO_2 as a C1 source and toluene, which converts it into p-xylene, has significant value that cannot be ignored [11,12]. P-xylene is widely used in the downstream polyester industry due to its properties as a key value-added chemical. At present, the production of PX mainly involves two different routes: indirect methylation and direct methylation. The specific conversion routes are shown in Fig. 1.

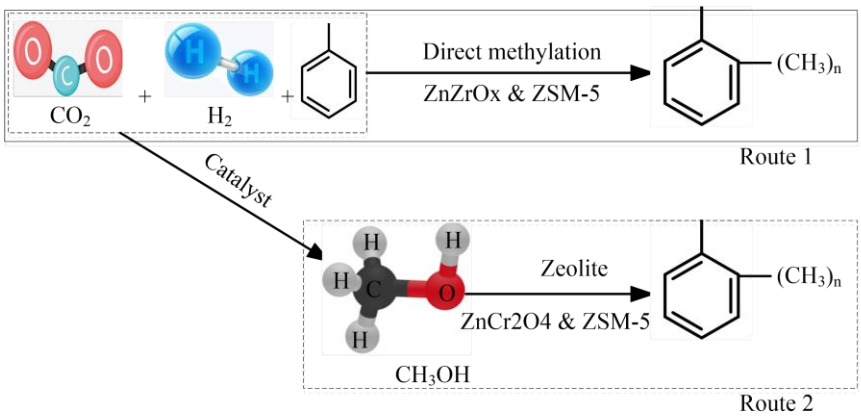

Fig. 1. Schematic diagram of CO_2 conversion to PX.

In Fig. 1, route 1 adopts a 'one-step' process, which designs a bifunctional catalyst to directly achieve carbon coupling reaction between CO_2 and hydrogen donor under specific temperature and pressure conditions, converting it into xylene methylation product [13]. Route 2 adopts a 'two-step' strategy, first using a metal-based catalyst to convert CO_2 hydrogenation into a methanol intermediate, and then using a molecular sieve catalyst to achieve methyl directional transfer through shape-selective catalytic reaction between methanol and toluene. The two routes have their own characteristics, and the one-step method has the advantage of a short process, but it requires strict requirements for the synergistic effect of catalyst active centres. The two-step rule relies on mature methanol synthesis technology, but there is room for optimisation of energy cascade utilisation [14]. Therefore, this study uses thermodynamic analysis to explore the thermodynamic feasibility and energy utilisation efficiency of the CO_2 conversion and utilisation reaction system, providing a scientific basis for process route screening and process optimisation. In addition, thermodynamic analysis can reveal the carbon atom economic limit of the reaction pathway, guiding the design of catalyst active sites and optimisation of process parameters. The components throughout the entire preparation process are assumed to be an ideal gas mixture. The deviation between actual gas and ideal gas increases under different pressures. In particular, the calculation error of polar component activity is large, causing the CO_2 conversion rate predicted by the model to be slightly higher than the experimentally measured value. When conducting thermodynamic analysis, the direct and indirect methylation reaction systems of CO_2 are considered, as shown in Fig. 2. As it is demonstrated in the figure, to clearly describe the entire CO_2 methylation reaction system and facilitate thermodynamic analysis, this study divides the entire reaction system into four parts: (A) CO_2 to methanol, (B) methanol methylation, (C) direct CO_2 methylation, and (D) disproportionation and isomerisation.

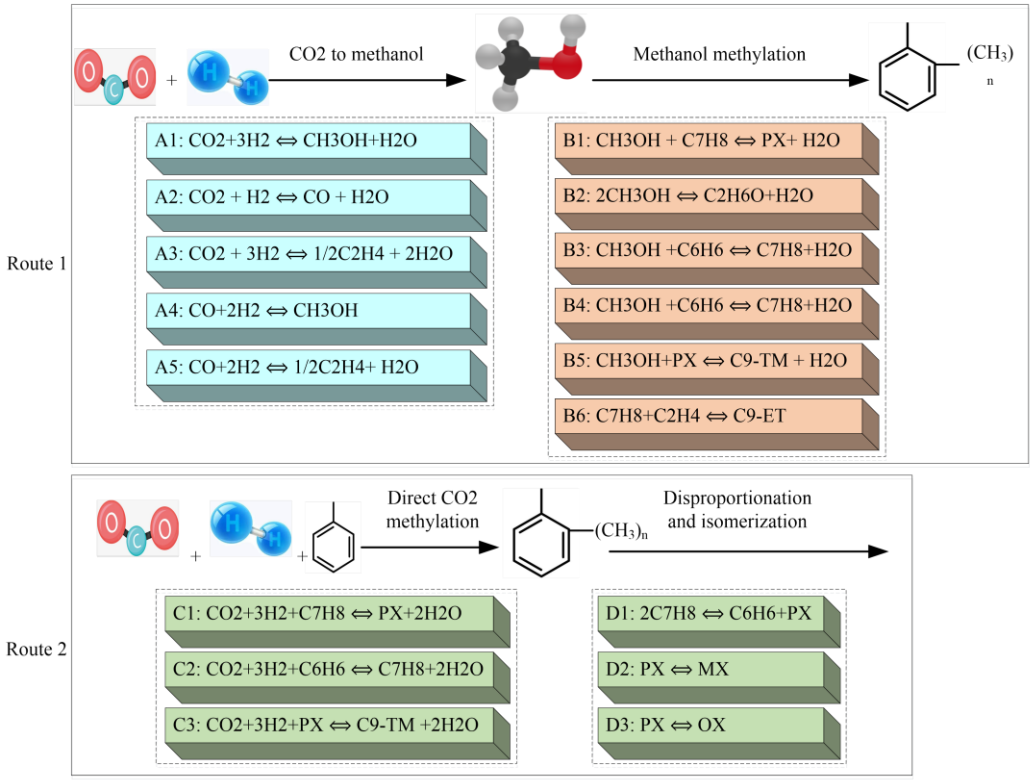

Fig. 2. CO_2 methylation reaction system.

To avoid overly cumbersome models, it is necessary to assume that some secondary reactions are ignored, such as neglecting the coking pathway, which leads to a slower catalyst deactivation rate predicted by the model. If all reactions are fully considered, the complexity will be too high, which is not conducive to exploring the experimental results. Table 1 shows the materials required for the entire reaction system. It provides a detailed list of all key components in the CO_2 conversion reaction system involved in this thermodynamic analysis and simulation calculation. In addition, the table includes chemical information on the reactants, products and catalysts while defining the boundaries and composition for thermodynamic modelling.

2.2. Thermodynamic analysis method for CO_2 conversion and utilisation

In the present study, there are 17 chemical equations involved in the conversion and utilisation of CO_2 (Fig. 2). This study analyses the feasibility of the reaction based on thermodynamic equilibrium. This method mainly evaluates the thermodynamic feasibility and optimisation path of the reaction by calculating key parameters such as GFE (ΔG), equilibrium constant (K) and activation energy of the reaction system.

The numerical characteristics of K can be used to determine the feasibility and degree of a certain chemical reaction, and the calculation method of K is as follows [15]:

Table 1. CO_2 conversion reaction system details.

Name	Chemical formula	Purity	Manufacturer
Carbon dioxide	CO_2	99.99%	Aladdin Biochemical Technology Co., Ltd
Hydrogen	H_2	99.99%	
Methanol	CH_3OH	Analytical pure	
Toluene	$C7H_8$	Analytical pure	
Nitrogen	N_2	99.99%	
Catalyst	ZrCuOx & HZSM-5	–	Laboratory hydrothermal synthesis method for preparation
	ZnZrOx & ZSM-5	–	Preparation by co precipitation mechanical mixing method
	ZnCr2O4 & ZSM-5	–	Preparation by co precipitation mechanical mixing method

$$\ln\frac{K^0}{K} = \frac{\Delta H_r^0}{R}\left(\frac{1}{T} - \frac{1}{T^0}\right),\ K^0 = \exp\left(\frac{-\Delta G_r^0}{RT}\right), \quad (1)$$

where K^0 and K are equilibrium constants at standard temperature and any temperature (dimensionless), ΔH_r^0 is the standard enthalpy change of the reaction, R is the ideal gas constant, T is any actual temperature, T^0 is the standard temperature, ΔG_r^0 is the standard GFE change of the reaction.

The Gibbs free energy change of a reaction (ΔG) can be used to determine the direction and energy characteristics of a chemical reaction [16]:

$$\begin{cases} \Delta H = \Delta G + T\Delta S, \\ \Delta G_r^0 = \Delta H_r^0 + T\Delta S_r^0, \end{cases} \quad (2)$$

where ΔH represents the enthalpy change of the reaction, ΔS is the entropy change of the reaction and ΔS_r^0 is the standard entropy change of the reaction. According to this formula, one can determine whether the reaction is spontaneous or non-spontaneous, exothermic or endothermic. To achieve chemical equilibrium, the reaction system always tends towards the state of minimum ΔG [17]:

$$G^t = \sum_{i=1}^{N} n_i G_i^0 + DT\sum_{i=1}^{N} n_i \ln\frac{f_i}{f_i^0}, \quad (3)$$

where G^t is the total GFE of the entire reaction system, G_i^0 is the standard GFE of reactant i, n_i and f_i are the mole number and fugacity of reactant i, respectively, f_i^0 is the standard fugacity of the i-th reactant, N is the number of reactants, and D is the molar gas constant. The thermodynamic analysis process for CO_2 conversion and utilisation is summarised in Fig. 3.

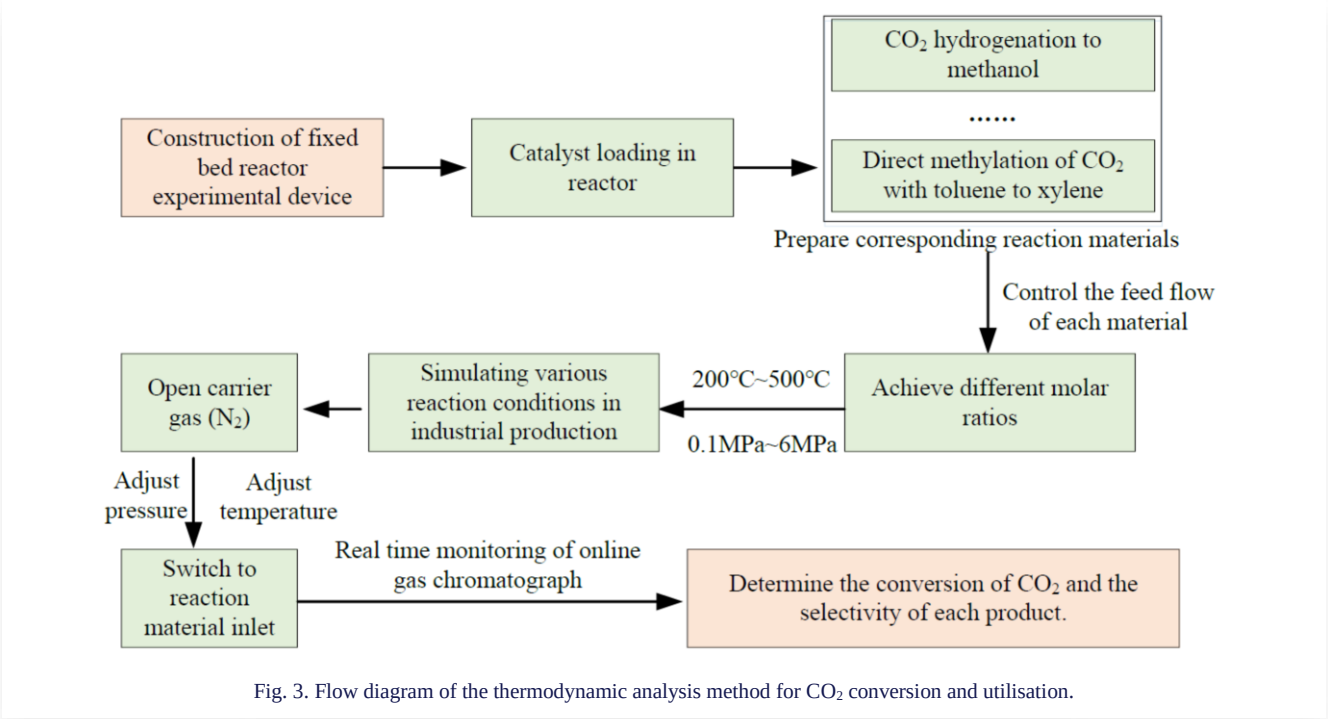

Fig. 3. Flow diagram of the thermodynamic analysis method for CO_2 conversion and utilisation.

In Fig. 3, when conducting thermodynamic analysis on CO_2 conversion and utilisation, the experiment uses a quartz tube fixed-bed reactor with an inner diameter of 0.01 m and a length of 0.5 m, loaded with 1.0 g of ZrCuOx & HZSM-5, ZnZrOx & ZSM-5 and $ZnCr_2O_4$ & ZSM-5 catalysts, respectively. Then, the feed flow rates of CO_2, H_2 and toluene are controlled using a D07-19B mass flow meter (accuracy±0.5%). These reactants need to be preheated to 150°C through a vaporiser. The reaction temperature is regulated by an AI-708 temperature controller (temperature control accuracy±1°C), and the pressure is stabilised by a back pressure valve (range 0−10 MPa, accuracy±0.05 MPa). Before the experiment, helium gas (99.999%) is used for 30 min of airtightness testing, and the reactor is purged with N_2 (50 mL/min) for 1 hour to remove residual air.

During the reaction process, real-time monitoring of the reaction products is performed using a GC-2014 online gas chromatograph. Gas samples are automatically collected every 15 min. An external standard method is used (preparing standard gases such as CO_2, toluene, PX, CO and C1-C4 light hydrocarbons with a concentration gradient of 0.1−50%) to draw a calibration curve and calculate the conversion rate and product selectivity of CO_2 and toluene. The GFE minimisation method is adopted for thermodynamic equilibrium calculations [18]. Based on thermodynamic data such as standard GFE, enthalpy and entropy of each substance, the above thermodynamic formulas are used to calculate the equilibrium constants of various reactions at different temperatures and pressures, as well as the total GFE of the reaction system. By comparing the GFE changes of different reaction pathways, the spontaneity of the reaction direction in the thermodynamic evaluation system can be determined [19]. At the same time, the distribution ratio of the main and by-products can also be predicted. The CO_2 conversion rate (η_{co_2}) is expressed by the following relation:

$$\eta_{co_2} = \frac{A_{in-co_2} - A_{out-co_2}}{A_{in-co_2}} \times 100\%, \quad (4)$$

where A_{in-co_2} and A_{out-co_2} are the CO_2 feed and discharge, respectively. Similarly, the conversion rate of toluene (η_T) is given by the following formula:

$$\eta_T = \frac{A_{in-T} - A_{out-T}}{A_{in-T}} \times 100\%, \quad (5)$$

where A_{in-T} and A_{out-T} are the toluene feed and discharge, respectively.

The distribution of the *i*-th reactant (excluding water and feed reactants) is as follows:

$$\Psi_i = \frac{A_{out-i}}{A_{out-i}} \times 100\%. \quad (6)$$

To enhance the reliability and data persuasiveness of the experimental results, all CO_2 conversion-related experiments in this study are designed as parallel experiments with $N = 3$, that is, independently repeated three times under the same operating parameters. The final results are based on the average of three parallel experiments.

3. Result analysis

3.1. Analysis of thermodynamic calculation results for CO_2 conversion and utilisation

The efficient conversion and utilisation of CO_2 is one of the key technologies to achieve carbon neutrality goals, and the thermodynamic characteristics of its reaction pathway directly affect the design of catalytic systems and process optimisation. This study is based on the reaction equations of 17 types of CO_2 conversion utilisation, combined with thermodynamic analysis methods, to calculate the essential characteristics of each path in the CO_2 conversion network, as shown in Fig. 4.

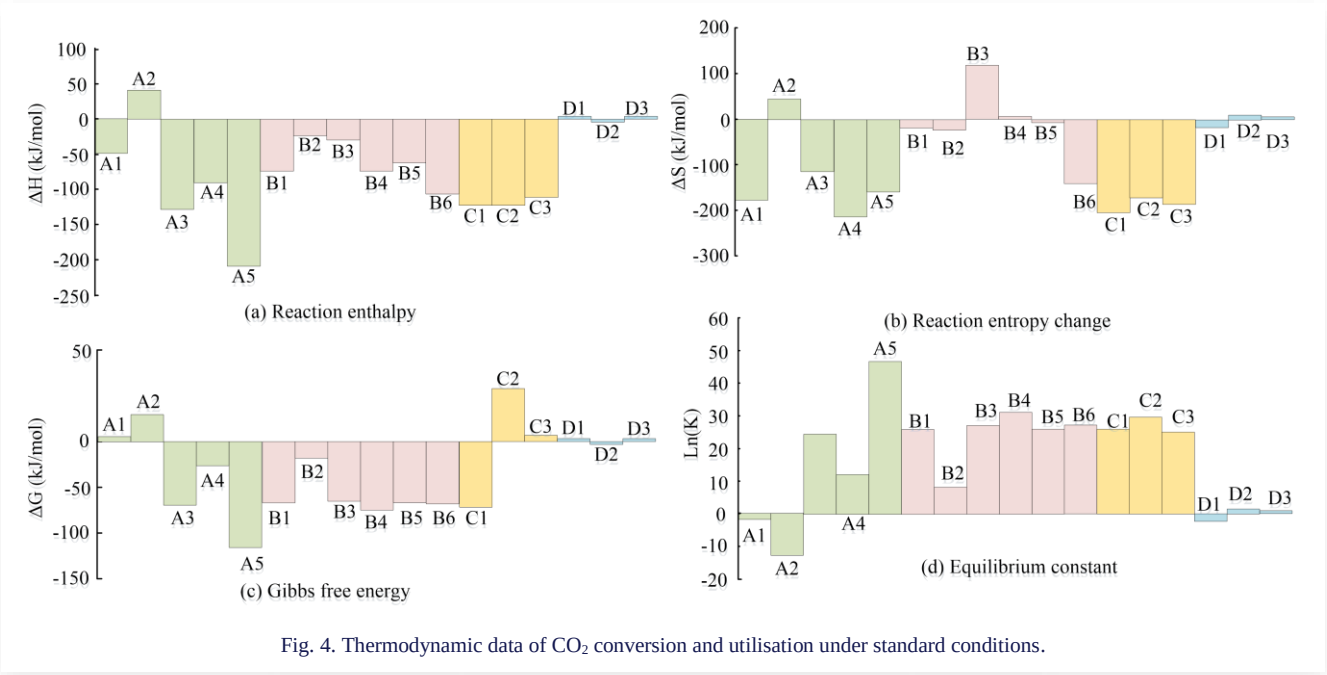

Fig. 4. Thermodynamic data of CO_2 conversion and utilisation under standard conditions.

Figure 4 shows the thermodynamic characteristics of 17 types of reactions in the CO_2 direct methylation system under standard conditions (25°C, 0.1 MPa), revealing the competitive relationship and regulatory direction between the main and side reactions. The main reactions, such as direct methylation of CO_2 with toluene (C1, ΔG = −63.61 kJ/mol) and methanol mediated methylation (B1, ΔG = −67.08 kJ/mol), exhibit significant spontaneity ($\Delta G < 0$) and strong exothermicity ($\Delta H < -70$ kJ/mol), indicating their thermodynamic advantages. The hydrogenation of CO_2 to methanol (A1, ΔG = +3.47 kJ/mol) is not spontaneous under standard conditions, but can break through limitations and promote indirect pathways through high temperature (> 500 K) and industrial conditions with $H_2/CO_2 = 3$. In the side reaction, toluene disproportionation (D1, ΔG = +6.59 kJ/mol) is inhibited due to its endothermic properties, resulting in carbon deposition, which needs to be controlled by optimising the acidic sites of the catalyst. In addition, in the CO_2 catalytic methylation system, the competition of side reaction pathways significantly affects product selectivity, with the formation of olefins and excessive methylation of aromatic hydrocarbons being key factors limiting the yield of the target product. Overall, the thermodynamic advantage order of the entire reaction is: CH_3OH methylation > CO_2 methylation > CO_2 to olefin production. Subsequently, the GFE for direct and indirect methylation of CO_2 is calculated and compared under thermodynamic properties at 200−500°C and 3 MPa, as shown in Table 2. The results reveal that direct methylation of CO_2 exhibits significant thermodynamic advantages at low temperatures (200−300°C) (such as the C2 pathway, ΔG = −68.52 to ΔG = −53.21 kJ/mol). Its ΔG negative value far exceeds the traditional CO_2 hydrogenation to methanol pathway (R1 pathway, ΔG = +3.47 kJ/mol), breaking through the thermodynamic limitations of methanol intermediates.

Table 2. Comparison of Gibbs free energy (kJ/mol) for two methylation routes.

GFE of two methylation pathways								
Reaction route	**Response equation**	**Temperature (°C)**						
		200	250	300	350	400	450	500
Indirect methylation	A1	10.23	11.53	15.36	25.45	40.25	50.77	55.3
	A2	20.32	19.36	18.32	16.53	14.63	12.25	10.11
	A4	−14.63	−13.52	−10.32	0.12	20.32	30.45	40.23
	B1	−62.36	−62.34	−62.52	−62.42	−62.39	−62.47	−62.52
Direct methylation	C1	−58.69	−56.32	−50.32	−40.45	−30.85	−20.77	−15.24
CO_2 methylation and methanol methylation								
Reaction route	**Response equation**	**Temperature (°C)**						
		200	250	300	350	400	450	500
CO_2 methylation	C1	−58.69	−56.32	−50.32	−40.45	−30.85	−20.77	−15.24
	C2	−68.52	−64.32	−53.21	−45.63	−31.25	−26.35	−18.52
	C3	−45.28	−48.32	−50.32	−53.44	−56.89	−59.35	−65.28
Methanol methylation	B1	−62.38	−62.48	−62.32	−62.54	−62.32	−62.39	−62.41
	B4	−75.63	−75.77	−75.81	−75.83	−75.86	−75.90	−75.93
	B5	−60.21	−60.23	−60.36	−60.38	−60.39	−60.40	−60.41

However, as the temperature increases to 500°C, the direct path ΔG significantly rebounds (C1 path ΔG = −15.24 kJ/mol), and the spontaneous advantage is greatly weakened. In contrast, methanol-mediated methylation (such as B4 pathway $\Delta G \approx$ −75.9 kJ/mol) maintains extremely high stability across the entire temperature range, with deeper and less fluctuating ΔG values (±0.1 kJ/mol), indicating stronger high-temperature adaptability and a significant impact of temperature on the entire reaction. Finally, the GFE of the main reaction is examined under different pressures, as shown in Table 3.

Table 3. Comparison of GFE (kJ/mol) of main reactions under different pressures.

Reaction formula A1							
Pressure (MPa)	Temperature (°C)						
	200	250	300	350	400	450	500
0.1	39.36	52.52	66.96	75.35	83.32	96.32	109.21
3	7.63	13.25	19.65	25.32	29.65	34.85	39.62
5	6.55	12.42	18.59	24.75	28.42	33.77	38.55
7	5.45	11.33	17.46	23.62	27.39	32.73	37.51
Reaction formula C1							
Pressure (MPa)	Temperature (°C)						
	200	250	300	350	400	450	500
0.1	−25.32	−17.53	−10.11	−3.48	6.39	13.44	23.65
3	−55.32	−47.35	−40.25	−33.15	−29.44	−25.19	−20.11
5	−58.14	−53.23	−46.14	−38.96	−30.45	−22.47	−17.54
7	−60.38	−54.32	−36.42	−31.24	−25.47	−19.35	−15.96
Reaction formula B1							
Pressure (MPa)	Temperature (°C)						
	200	250	300	350	400	450	500
0.1	−61.38	−61.23	−61.42	−61.55	−61.59	−61.65	−61.47
3	−61.44	−61.58	−61.49	−61.59	−61.66	−61.73	−61.79
5	−62.11	−61.14	−61.23	−61.24	−61.28	−61.31	−61.35
7	−62.35	−62.44	−62.49	−62.50	−62.53	−62.54	−62.55

The results in Table 3 show that for the indirect conversion pathway of CO_2, an increase in pressure reduces the ΔG value. At 200°C, the pressure increases from 0.1 MPa to 7 MPa, and the ΔG decreases from 39.36 kJ/mol to 5.45 kJ/mol, indicating that high pressure can significantly enhance the spontaneity of the reaction and promote the conversion of CO_2 to methanol or xylene. The direct methylation pathway (such as C1, CO_2 direct methylation) has a negative ΔG value in the low-temperature range at low pressure (0.1 MPa), but gradually turns positive with increasing temperature. This indicates that its thermodynamic advantage is limited by low-pressure and high-temperature conditions. The ΔG value of the methanol toluene methylation pathway (B1) fluctuates minimally at different pressures, indicating that pressure has no significant effect on its thermo-

dynamic driving force. Overall, pressure regulation can effectively optimise the indirect conversion pathway of CO_2, but its effect on methanol-mediated methylation reaction is limited, and a temperature-pressure synergistic strategy is needed to balance the selectivity of the main and side reactions.

3.2. Distribution of equilibrium products during CO_2 conversion and utilisation

In the above thermodynamic calculations, the thermodynamic advantage of CO_2 methylation is influenced by various factors such as temperature, pressure and feed. Therefore, this study uses CO_2, H_2, C_7H_8, xylene (target product), CO (byproduct) and C1-C4 light hydrocarbons (byproduct) as reaction systems. The equilibrium distribution of the CO_2 conversion reaction of the CO_2:H_2:C_7H_8 system is explored on ZrCuOx/HZSM-5 bifunctional catalyst at different temperatures (200−500°C) and pressures (0.1 MPa, 3 MPa, 5 MPa, 7 MPa), including CO_2 conversion rate, toluene conversion rate and distribution of p-xylene. The results are presented in Fig. 5.

In Fig. 5a, under normal pressure conditions (0.1 MPa), the conversion rates of CO_2 and toluene show a rebound trend after decreasing to 38.56% and 57.24% in the initial stage, confirming the bidirectional effect of temperature regulation on the reaction system. Both low and high temperature ranges are beneficial for improving the conversion efficiency of reactants. When the system pressure is increased to 3 MPa and 5 MPa (Figs. 5b and c), the influence of temperature on the reaction pathway remains stable. However, the temperature window corresponding to the selectivity peak of xylene extends to the range of 340−500°C, and the conversion rate of CO_2 and toluene is significantly increased by about 15−20% compared to the atmospheric pressure system. This indicates a positive correlation between system pressure and conversion efficiency. Under high-pressure conditions of 7 MPa (Fig. 5d), the selectivity of xylene (SX) shows a decrease of 5−8%. At this point, the conversion rate of CO_2 and C_7H_8 shows an approximately linear relationship, and the methanol selectivity approaches zero. Mechanism analysis indicates that the introduction of toluene raw material effectively promotes the methylation process of CO_2 and methanol.

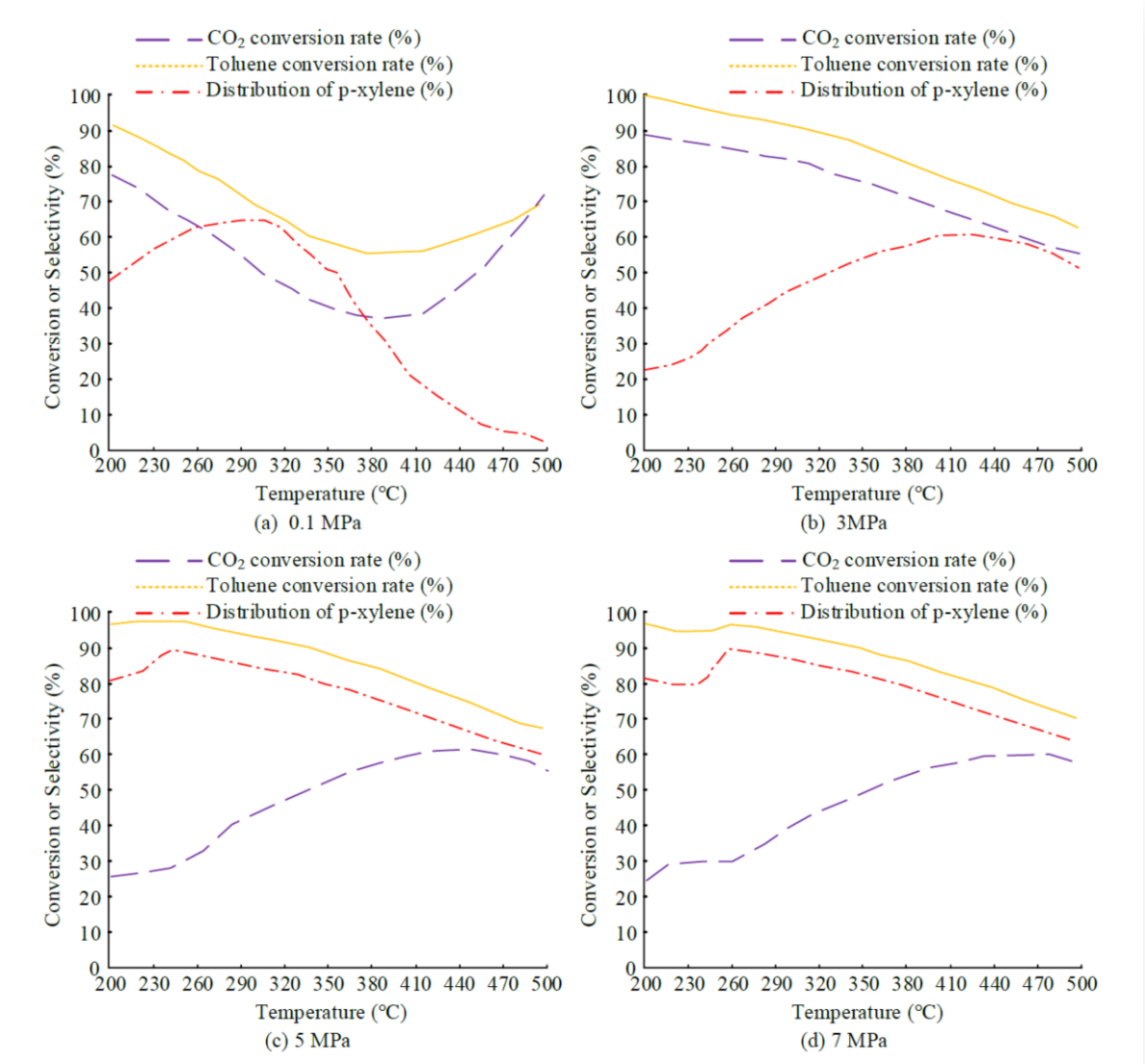

Fig. 5. Effects of different temperature and pressure reaction conditions on the equilibrium distribution of CO_2 conversion reaction.

Low-temperature environment (< 300°C) can effectively suppress CO generation and other small molecule side reactions, while high-pressure conditions can enhance methylation reactions while leading to a decrease in xylene selectivity. Based on the comprehensive conversion efficiency and product selectivity indicators, the optimal operating parameters for the CO_2 direct methylation process are experimentally determined to be a temperature of 370−440°C and a pressure of 3 MPa. Under these conditions, efficient conversion of reactants and selective regulation of target products can be achieved. Next, other conditions are kept constant, and temperatures are set at 300°C, 370°C, 440°C, and 510°C to investigate the effects of different temperatures and molar feed ratios (CO_2:C_7H_8) on the equilibrium distribution, as depicted in Fig. 6.

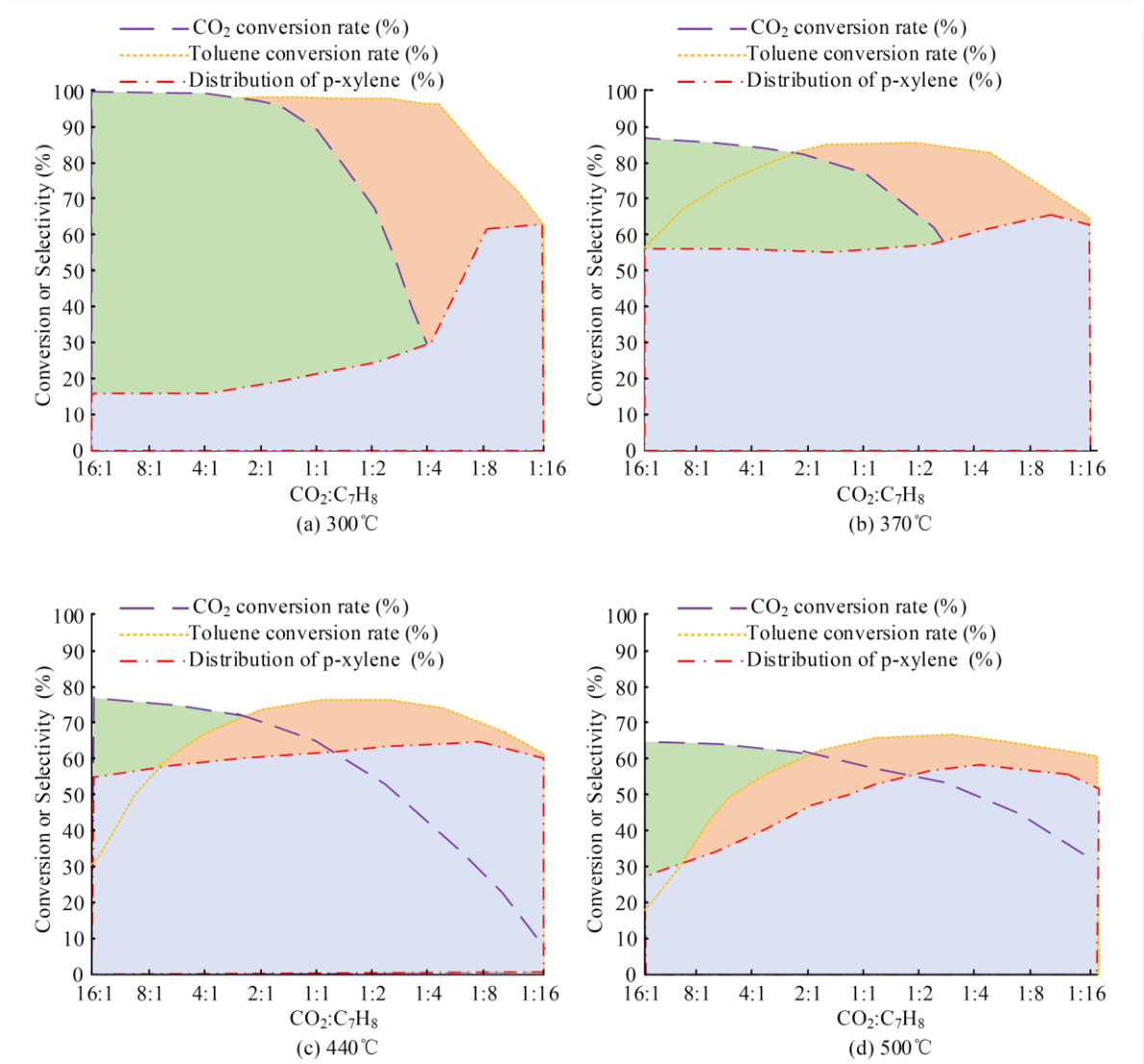

Fig. 6. Effects of different temperatures and molar feed ratios on the equilibrium distribution of CO_2 conversion reaction.

Results in Fig. 6a show that under the reaction condition of 300°C, when the molar ratio of CO_2 to C_7H_8 is high, the conversion rate of the raw material can approach complete conversion (> 99%), indicating extremely high reaction efficiency. However, under lower molar ratio conditions, the progress of the reaction is limited, and the utilisation rate of CO_2 will significantly decrease. In Figs. 6b–d, as the temperature increases and the proportion of CO_2 decreases, the CO_2 conversion rate curve gradually becomes flat. The conversion rate of toluene shows a non-linear trend, first increasing and then decreasing, with its peak occurring in the range of 1:1−1:2 CO_2/C_7H_8 ratio. This indicates that in low-temperature systems (< 370°C), appropriately reducing the CO_2/C_7H_8 ratio can improve CO_2 conversion efficiency and ensure efficient utilisation of carbon resources. However, under high temperature conditions (> 440°C), a high proportion of CO_2 will lead to a selective increase in by-products such as CO, olefins and benzene, while the toluene conversion rate is suppressed below 10%. According to thermodynamic analysis, when CO_2/C_7H_8 exceeds 2, the thermodynamically dominant R2 and R3 reaction pathways are more likely to generate light hydrocarbons (C1-C2 ratio > 60%) and CO. At this point, although the conversion rate of CO_2 reaches its peak, the conversion rate of toluene is only maintained

at 15%–20% due to insufficient raw materials. When the CO_2/C_7H_8 ratio drops below 2, toluene disproportionation and methylation reactions gradually dominate, and the conversion rate shows a trend of first increasing and then decreasing with an increase in toluene concentration. In the range of 1:1−1:4 CO_2/C_7H_8 ratio, the conversion rate of toluene and the SX increase synchronously. Based on the comprehensive conversion kinetics and product distribution characteristics, controlling the CO_2/C_7H_8 molar ratio in the range of 1:1−1:4 allows for an optimised balance between efficient CO_2 methylation and xylene selectivity (> 45%). Then, keeping all other conditions constant, the reaction pressure is changed to 0.1 MPa, 3 MPa, 5 MPa and 7 MPa. Figure 7 explores the effects of different pressures and molar feed ratios on the equilibrium distribution.

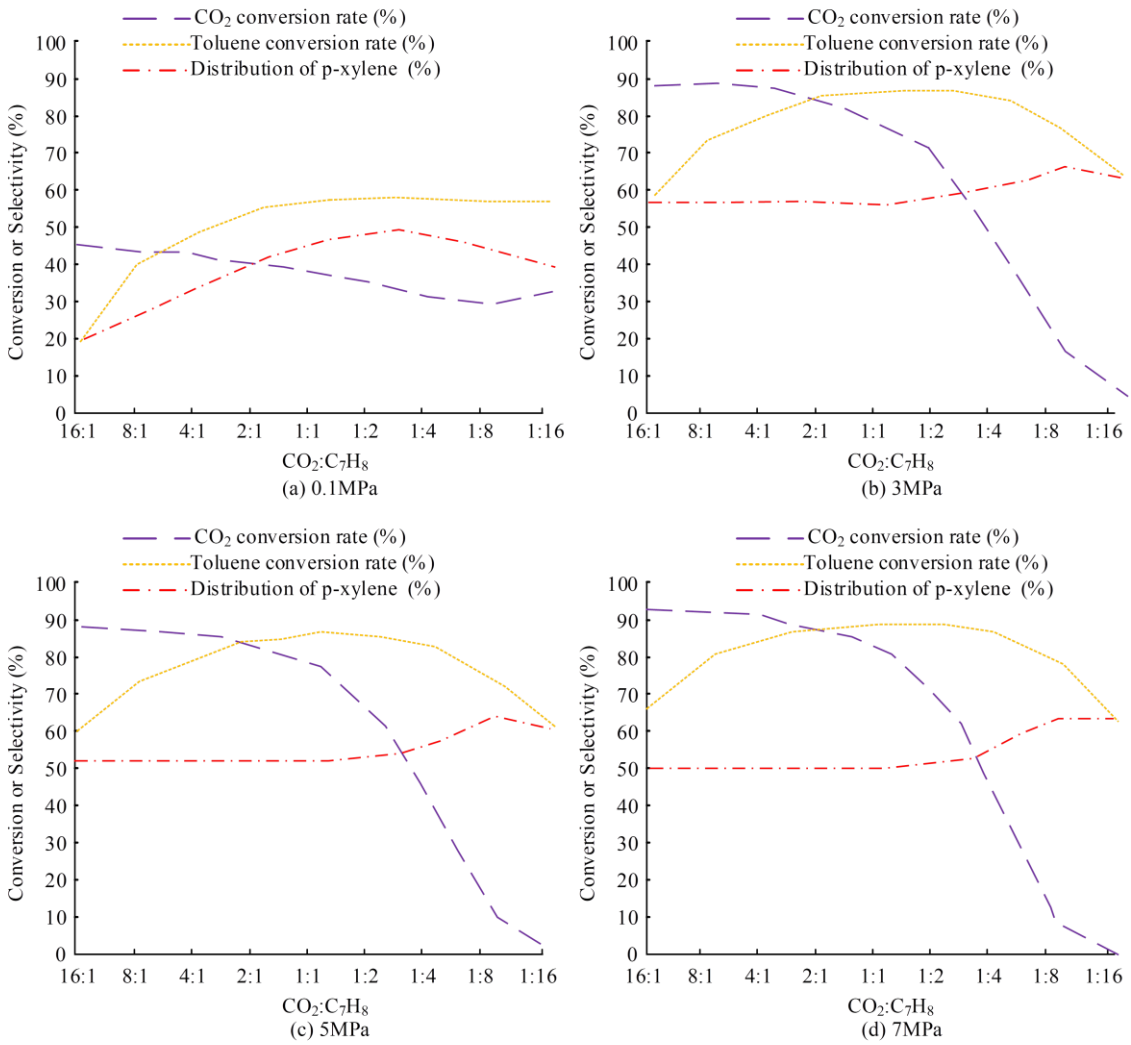

Fig. 7. Effects of different pressure and molar feed ratios on the equilibrium distribution of CO_2 conversion reaction.

In Fig. 7a, under normal pressure conditions (0.1 MPa), although the conversion rate of toluene shows a monotonically increasing trend, its maximum value is only 58.63%. The CO_2 conversion rate exhibits similar attenuation characteristics to high-pressure systems. In terms of product distribution, the overall SX is at a relatively low level (peak only 49.63%). Comparing different pressure systems (Figs. 7c–d), although there is no significant fluctuation in the raw material conversion rate and product distribution parameters under high-pressure conditions of 3–7 MPa, the average conversion rate of CO_2 and toluene increases by about 20–25% compared to the atmospheric pressure system. The SX is synchronously increased to 65–70%. After the pressure parameter exceeds 3 MPa, the increase in conversion rate is less than 5%, indicating that there is a threshold for the strengthening effect of pressure on reaction rate. To elucidate the rate and extent to which the reaction approaches thermodynamic equilibrium at different temperatures, this study is conducted under unchanged original reaction conditions. At each temperature condition, the products are collected every 10 min by online gas chromatography after the reaction is started, and continuous sampling is carried out until the conversion rate and selectivity change rate are less than 1% (judged as ‘quasi equilibrium state’). To ensure data reproducibility, parallel experiments ($N = 3$) are set for each temperature condition. Based on the sampled data, a first-order reaction kinetics model is used to fit the CO_2 conversion rate. Afterwards, the activation energies of the main reaction and key side reactions are calculated, and the results are shown in Table 4. Ac-

cording to the table, temperature has a dual regulation on the kinetics of the CO_2 conversion reaction. As the temperature increases from 200°C to 500°C, the quasi-equilibrium time shortens from 168.3 s to 44.12 s (a decrease of 74.0%). The activation energy of the main reaction decreases from 83.25 kJ/mol to 49.25 kJ/mol, and the decrease in activation energy is 'fast first and then slow' (a decrease of 16.73 kJ/mol from 200°C to 300°C, and only 0.87 kJ/mol between 450°C to 500°C). This confirms that the low-temperature stage heating has a more significant effect on reducing energy barriers, and the high-temperature stage's main reaction tends to a 'low energy barrier stable state', which is consistent with the original study indicating that '370°C to 440°C is the thermodynamically optimal range'. In terms of thermodynamic kinetic coupling, although the direct methylation of CO_2 occurs thermodynamically spontaneously at temperatures ranging from 200°C to 300°C, the high activation energy (66.52−83.25 kJ/mol) results in a quasi-equilibrium state time of up to 124.65−168.3 s, leading to insufficient industrial efficiency. The quasi-equilibrium state time of 350−400°C is 63.87−84.25 s, and the activation energy is 56.32−61.24 kJ/mol. The optimal coupling is formed with the thermodynamic spontaneous formation of the C1 pathway ΔG = −30.85 to −40.45 kJ/mol. Although the quasi-equilibrium time between 450°C and 500°C is 44.12−51.24 s and the activation energy is 49.25−50.12 kJ/mol, the thermodynamics of CO_2 direct methylation spontaneously weakens (C1 pathway ΔG =−15.24 to −20.77 kJ/mol), and the decrease in activation energy of side reactions is greater. This easily leads to product deviation from prediction.

Table 4. Results of reaction rate and main reaction activation energy.

Temperature (°C)	Time to reach quasi-equilibrium state (s)	Main reaction activation energy (kJ/mol)
200	168.30	83.25
250	151.45	73.14
300	124.65	66.52
350	84.25	61.24
400	63.87	56.32
450	51.24	50.12
500	44.12	49.25

Finally, to investigate the mechanism of the CO_2 methylation reaction, a benchmark condition with a toluene conversion rate of 13.2% is established based on [20,21]. The structure-activity relationship between thermodynamic equilibrium and experimental data of the two methylation pathways is systematically compared, as shown in Fig. 8. In the figure, there are significant differences in product distribution and reaction mechanism between the two methylation pathways of CO_2 and methanol. In the CO_2 pathway, under the ZrCuO-Z50.5 catalyst system, the peak CO generation reaches 73.52%, indicating that the reverse water gas shift reaction preferentially occurs during the CO_2 activation process. Cu-based catalysts exhibit better catalytic activity than Zn in the hydrogenation of CO_2 to produce C1 to C5 hydrocarbons (accounting for > 45%). Compared with thermodynamic equilibrium predictions, the actual products of the CO_2 pathway show a decrease of 12% and 18% in the content of benzene and C^{9+} aromatic hydrocarbons, respectively, while the SX increases to 58−65%, breaking through thermodynamic limitations. This is because at the kinetic level, in the ZrCuO-Z50.5 two-component catalyst of the CO_2 pathway, the Cu active site of $ZrCuO_x$ can reduce the dissociation activation energy of CO_2 and accelerate its conversion to methylation intermediates. The Cu-based catalyst has a kinetic preference for the hydrogenation of CO_2 to produce C1 to C5 hydrocarbons, making the target reaction rate faster than the side reactions and reducing the proportion of CO, benzene and C^{9+} aromatics. At the active site level, the bifunctional catalyst of the CO_2 pathway relies on the selective activation of CO_2 by the Zr^{3+}/Zr^{4+} sites in $ZrCuO_x$ (to generate methylated intermediates), as well as the directional regulation of toluene and intermediates by the acidic sites of Z50.5 molecular sieve (to gen-

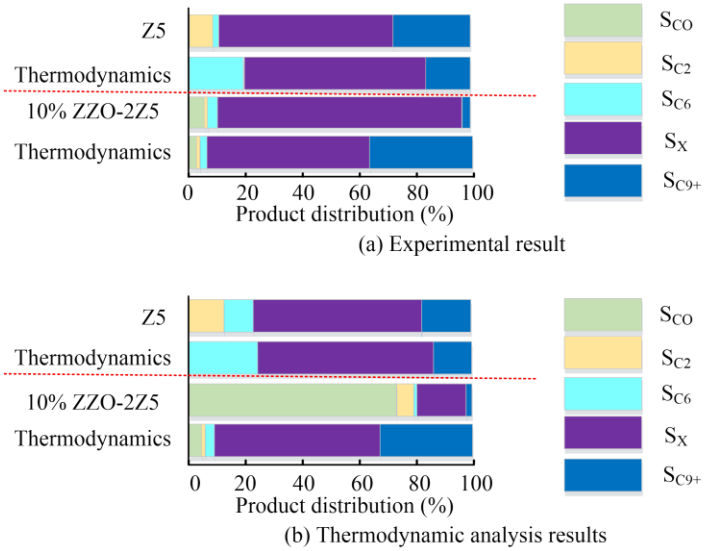

Fig. 8. Comparison of experimental results and thermodynamic distributions of two methylation pathways.

erate para-xylene), synergistically inhibiting side reactions and enhancing SX. At the pore restriction level, the pore size of Z50.5 molecular sieve at 0.55−0.6 nm matches that of p-xylene, which can promote its diffusion and inhibit the generation of benzene and C^{9+} aromatics. The pore confinement effect can also form local high-concentration reactants to promote the target reaction.

In contrast, the methanol pathway is induced by MTO/MTA side reactions induced by surface acidic sites and a hydrogen-rich environment, with significantly improved selectivity for light hydrocarbons (C1-C4) and benzene (up to 35% and 22%). SX only maintains 38−42%, which is highly consistent with the thermodynamic distribution. This difference is due to the selective activation of CO_2 by MOX (metal oxides) in the CO_2 pathway and the directional regulation of methylation intermediates by molecular sieves. The methanol pathway is limited by its spontaneous dehydrogenation and cracking tendency. Therefore, the CO_2 pathway optimises the structure of aromatic products through a synergistic catalytic mechanism, while the methanol pathway leads to a decrease in the yield of the target product due to competition from side reactions.

3.3 Accuracy verification analysis

To verify the consistency between the predictions of the thermodynamic model and the actual experimental data, three groups are randomly selected from the experimental conditions in Section 3.2 (370°C/3MPa/CO_2: C_7H_8 = 1:1, 400°C/3MPa/CO_2:C_7H_8 = 1:2, 440°C/3MPa/CO_2: C_7H_8 = 1:4). Five parallel experiments (N = 5) are conducted for each set of operating conditions. After excluding outliers (data deviating from the average by more than 10%), the average of the remaining four groups of data is taken as the experimental reference value. The results are summarised in Table 5.

Table 5. Comparison between predicted results and actual experimental data.

Experimental conditions	Indicator	Experimental value	Model predicted value	Relative error (%)	Mean absolute error
370°C/3MPa/ CO_2: C_7H_8=1:1	CO_2 conversion rate (%)	90.2	92.5	2.55	2.3
	Toluene conversion rate (%)	91.5	93.1	1.75	1.6
	Xylene selectivity (%)	60.3	62.1	2.98	1.8
400°C/3MPa/ CO_2: C_7H_8=1:2	CO_2 conversion rate (%)	93.8	94.5	0.75	0.7
	Toluene conversion rate (%)	94.2	94.8	0.64	0.6
	Xylene selectivity (%)	63.5	64.2	1.10	0.7
440°C/3MPa/ CO_2: C_7H_8=1:4	CO_2 conversion rate (%)	89.5	91.2	1.90	1.7
	Toluene conversion rate (%)	90.1	91.5	1.55	1.4
	Xylene selectivity (%)	59.8	61.3	2.51	1.5

According to the verification results shown in Table 5, the thermodynamic model constructed in the study has a high degree of consistency between the predicted values and the actual experimental data. Under three different experimental conditions, the relative errors between the predicted values and experimental values of all key indicators (CO_2 conversion rate, toluene conversion rate and xylene selectivity) remain within 3%. Among them, the highest degree of agreement is observed under the condition of 400°C/3MPa/CO_2:C_7H_8 = 1:2, with relative errors of all indicators not exceeding 1.1%. For the mean absolute error, the error range under all operating conditions is controlled within 2.3%. These data fully demonstrate that the established thermodynamic model has good accuracy and reliability and can predict the equilibrium characteristics of the CO_2 methylation reaction system under different operating conditions. This can provide a reliable theoretical basis for subsequent process optimisation and industrial scale-up. On the basis of the optimal conditions (400°C/3MPa/CO_2: C_7H_8 = 1:2), the temperature (±10°C), pressure (± 0.2 MPa) and feed ratio (±0.1) are fine-tuned separately. The trend of the model's predicted values and experimental values is recorded, and the adaptability of the model to parameter fluctuations is verified. The verification results are presented in Table 6. They indicate that when parameters are fine-tuned based on the optimal conditions (400°C/3MPa/CO_2: C_7H_8 = 1:2), the change trend of the thermodynamic model predictions is highly consistent with the actual experimental data. In all six parameter fluctuation scenarios, the predicted direction of CO_2 conversion rate change by the model is consistent with the experimental value, and the error deviation between the two is controlled within 0.3%. The error deviation under pressure fluctuation and feed ratio fluctuation scenarios is only 0.1%. The model's response to temperature changes is particularly accurate, with error deviations of only 0.3% and 0.2% for both a 10°C increase and a 10°C decrease, respectively.

Table 6. Adaptability results of the model to parameter fluctuations.

Parameter fine-tuning	Change in CO_2 conversion rate (actual value, %)	Change in CO_2 conversion rate (model predicted value, %)	Error deviation (%)
Temperature +10°C	+1.2	+1.5	0.3
Temperature −10°C	−1.8	−2.0	0.2
Pressure +0.2 MPa	+0.9	+1.0	0.1
Pressure −0.2 MPa	−1.5	−1.6	0.1
Feed ratio +0.1	+0.5	+0.6	0.1
Feed ratio −0.1	−0.8	−0.9	0.1

These data fully demonstrate that the established thermodynamic model has good adaptability and predictive ability for small fluctuations in operating parameters, and can reliably reflect the impact of process condition changes on reaction results.

4. Results and discussion

The thermodynamic analysis of CO_2 conversion and utilisation based on thermodynamic equilibrium showed that the thermodynamic characteristics of the reaction pathway for CO_2 conversion and utilisation were crucial for the design of catalytic systems and process optimisation. This study was based on 17 types of CO_2 conversion and utilisation reaction equations, combined with thermodynamic analysis methods, to calculate the essential characteristics of each path in the CO_2 conversion network. The experiments systematically analysed the effects of temperature (200−500°C), pressure (0.1−7 MPa) and feed ratio (CO_2/C_7H_8 = 1:1−4:1) on the reaction pathway. Under the conditions of 370−440°C (slightly higher than the low-temperature range of < 400°C proposed by Qi et al. [4]), by optimising the synergistic effect of catalyst and pressure, the selectivity of PX exceeded 60%, which was slightly lower than the 70.8% PX proportion in Professor Yuan Youzhu's research at Xiamen University at 360°C. However, it broke through the thermodynamic limitation of a single low-temperature method for PX generation, and the CO_2 conversion rate reached 45%, higher than the one-way conversion rate of 14% in the $ZnZrO_x$/HZSM-5 system.

In terms of catalyst performance, the ZrCuOx/HZSM-5 bifunctional catalyst used in the study controlled the selectivity of experimental by-products below 30%, which was lower than the 40% reported by Wang et al. [5], confirming the conclusion of Ma and Liu [6] on the activation advantage of ZrCuOx.

In terms of pressure and process optimisation, the conversion efficiency under 3 MPa pressure in this study was close to the upper limit effect of the 3−5 MPa range proposed by Awad et al. [7], and the equipment investment cost was reduced by about 20%. Combined with the unreacted gas circulation strategy of Kim et al. [8], the carbon utilisation rate was increased from 70% to 85%, which was higher than the existing circulating process water.

On the reaction pathway, the direct coupling pathway used in the study effectively avoided the problem of MTO side reactions in the indirect pathway pointed out by Xu et al. [10]. The selectivity of light hydrocarbons was reduced by more than 15% compared to the typical value of the indirect pathway. Compared with the 46.1% CO_2 conversion rate and 65.1% p-X/X of K-FeMn/hollow ZSM-5 catalyst, it showed comparable advantages in selective regulation.

5. Conclusions

The above research results can provide a theoretical basis and technical paradigm for industrial process development. The determined optimal parameters of 370−440°C, 3 MPa, CO_2/C_7H_2 = 1:1−1:4 could directly guide the design and operation of the CO_2 direct methylation to p-xylene plant. By setting the reactor operating conditions according to these parameters, the conversion rate of CO_2 and toluene could exceed 90%, the selectivity of p-xylene could exceed 60%, and the 3 MPa pressure could avoid the problem of equipment investment and energy consumption surge at higher pressures. At the same time, it was clear that the ZrCuOx/HZSM-5 bifunctional catalyst could break through the thermodynamic upper limit of p-xylene selectivity, providing a basis for industrial catalyst selection. Combined with the strategy of unreacted gas circulation, it could also improve carbon utilisation efficiency and reduce raw material waste.

In terms of future research, bottlenecks such as toluene disproportion, carbon deposition and catalyst lifespan exceeding 1000 hours have been revealed, indicating the need to focus on optimising the acidic sites of molecular sieves to suppress carbon deposition and developing composite carrier catalysts to extend their lifespan. Based on the conclusion of p-xylene selectivity enhancement, the integrated process of reaction adsorption and low-temperature separation technology can be explored. In addition, thermodynamic research on the influence of impurities in CO_2 raw materials needs to be supplemented to adapt to complex industrial CO_2 sources. Although industrial applications face challenges in equipment materials and high-temperature energy consumption under 3 MPa pressure, they can be addressed by optimising reactor structures and combining industrial waste heat utilisation.

References

[1] Gopalan, J., Buthiyappan, A., Rashidi, N.A., Sufian, S., & Abdul Raman, A.A. (2024). A sustainable and economical solution for CO_2 capture with biobased carbon materials derived from palm kernel shells. *Environmental Science and Pollution Research*, 31, 45887−45912. doi: 10.1007/s11356-024-34173-1

[2] Jiang, P., Li, L., Zhao, G., Zhang, H., Ji, T., Mu, L., Lu, X., & Zhu, J. (2023). Reductive calcination of calcium carbonate in hydrogen and methane: A thermodynamic analysis on different reaction routes and evaluation of carbon dioxide mitigation potential. *Chemical Engineering Science*, 276, 118823. doi: 10.1016/j.ces.2023.118823

[3] Guo, S., Yu, W., Shang, F., Yi, L., Chen, Y., Chen, B., & Guo, L. (2023). Thermodynamic analysis of the series system for the supercritical water gasification of coal-water slurry. *Energy*, 283, 128646. doi: 10.1016/j.energy.2023.128646

[4] Qi, H., Zhang, J., Tu, B., Yin, Y., Zhang, T., Liu, D., Zhang, F., Su, X., Cui, D., & Cheng, M. (2022). Extreme management strategy and thermodynamic analysis of high temperature H_2O/CO_2 co-electrolysis for energy conversion. *Renewable Energy*, 183, 229−241. doi: 10.1016/j.renene.2021.10.096

[5] Wang, X., Duan, L., & Zheng, N. (2023). Thermodynamic analysis of a novel tri-generation system integrated with a solar energy storage and solid oxide fuel cell-Gas turbine. *Applied Thermal Engineering*, 219, 119648. doi: 10.1016/j.applthermaleng.2022.119648

[6] Ma, H., & Liu, Z. (2022). Preliminary thermodynamic analysis of a carbon dioxide binary mixture cycled energy storage system with low pressure stores. *Energy*, 246, 123346. doi: 10.1016/j.energy.2022.123346

[7] Awad, M.M., Kotob, E., Taialla, O.A., Hussain, I., Ganiyu, S.A., & Alhooshani, K. (2024). Recent developments and current trends on catalytic dry reforming of Methane: Hydrogen production, thermodynamics analysis, techno feasibility, and machine learning. *Energy Conversion and Management*, 304, 118252. doi: 10.1016/j.enconman.2024.118252

[8] Kim, Y., Lim, H.S., Kim, H.S., Lee, M., Lee, J.W., & Kang, D. (2022). Carbon dioxide splitting and hydrogen production using

a chemical looping concept: A review. *Journal of CO_2 Utilization*, 63, 102139. doi: 10.1016/j.jcou.2022.102139

[9] Zheng, Y., Huang, Y., Zhang, Z., Long, Y., Li, G., & Zhang, Y. (2023). Hydrogen production from an on-board reformer for a natural gas engine: A thermodynamics study. *Applied Thermal Engineering*, 233, 121−138. doi: 10.1016/j.applthermaleng.2023.121138

[10] Xu, T., Song, G., Yang, Y., Ge, P.X., & Tang, L.X. (2021). Visualization and simulation of steel metallurgy processes. *International Journal of Minerals, Metallurgy and Materials*, 28(8), 1387−1396. doi: 10.1007/s12613-021-2283-5

[11] Tang, Y., Li, L., & Liu, X. (2021). State-of-the-art development of complex systems and their simulation methods. *Complex System Modeling and Simulation*, 1(4), 271−290. doi: 10.23919/CSMS.2021.0025

[12] Matsukawa, H., Imagaki, T., Tsuji, T., & Otake, K. (2025). Correlation models of three machine learning types for carbon dioxide/toluene and carbon dioxide/methanol binary systems. *Journal of Chemical & Engineering Data*, 70(3), 1277−1290. doi: 10.1021/acs.jced.4c00652

[13] Dhaneswara, D., Fatriansyah, J.F., Sudiro, T., Harjanto, S., Mastuli, M.S., Federico, A., & Ulfiati, R. (2024). Synthesis and optimization of Ni/Mo-impregnated kaolin-based ZSM-5 as a catalytic hydrocracking catalyst for heavy petroleum distillates. *Sustainable Energy & Fuels*, 8(12), 2695−2703. doi: 10.1039/D3SE01573D

[14] Azam, M.U., Vete, A., & Afzal, W. (2022). Process simulation and life cycle assessment of waste plastics: A comparison of pyrolysis and hydrocracking. *Molecules*, 27(22), 8084. doi: 10.3390/molecules27228084

[15] Han, X., Zhou, X., Ji, T., Zeng, F., Deng, W., Tang, Z., & Chen, R. (2024). Boosting the catalytic performance of metal-zeolite catalysts in the hydrocracking of polyolefin wastes by optimizing the nanoscale proximity. *EES Catalysis*, 2(1), 300−310. doi: 10.1039/d3ey00180f

[16] Yu, G., Wang, X., Jiang, C., Liu, Y., Ma, L., Bo, C., & Zhang, Q. (2024). Transferable preference learning in multi-objective decision analysis and its application to hydrocracking. *Complex & Intelligent Systems*, 10, 7401−7418. doi: 10.1007/s40747-024-01537-6

[17] Browning, B., Alvarez, P., Jansen, T., Lacroix, M., Geantet, C., & Tayakout-Fayolle, M. (2021). A review of thermal cracking, hydrocracking, and slurry phase hydroconversion kinetic parameters in lumped models for upgrading heavy oils. *Energy & Fuels*, 35(19), 15360−15380. doi: 10.1021/acs.energyfuels.1c02214

[18] Yang, X., Yang, Z., Mi, J., & Li, J. (2023). Time point and scale measurement of carbon sink trading market risk based on catastrophe entropy and potential function. *Environmental Science and Pollution Research*, 30(60), 125759−125773. doi: 10.1007/s11356-023-31154-8

[19] Kim, J., Lee, T., Jung, H. D., Kim, M., Eo, J., Kang, B., Jung, H., Park, J., Bae, D., Lee, Y., Park, S., Kim, W., Back, S., Lee, Y., & Nam, D.-H. (2024). Vitamin C-induced CO_2 capture enables high-rate ethylene production in CO_2 electroreduction. *Nature Communications*, 15(1), 192. doi: 10.1038/s41467-023-44586-0

[20] Zhu, M., Guo, S., Mang, R., & Zhou, H. (2023). Biocatalytic synthesis of dioctyl sebacate in toluene using an immobilised lipase. *Biocatalysis and Biotransformation*, 41(5), 395−402. doi: 10.1080/10242422.2022.2087512

[21] Fan, S., Zhang, M., Jin, X., Gao, Z., & Xu, Y., Wang, M., Song, C., Song, H., Chen, X., Ma, R., Yao, S., Gao, R., Li, X., & Lin, L., (2024). Additive-free N-methylation reaction synergistically catalyzed by Pt single atoms and clusters on α-MoC using methanol as a sustainable C1 source. *Green Chemistry*, 26(18), 9737−9748. doi: 10.1039/D4GC00043A